Electronic Supplementary Information (ESI†)

Rhodamine phenol-based fluorescent probe for visual detection of GB and its simulant DCP

Shouxin Zhang [a], Chuan Zhou [a], Bo Yang [a], Yue Zhao [a], Lingyun Wang [a],

Bo Yuan [a, b], Heguo Li [a,*]

[a]State Key Laboratory of NBC Protection for Civilian, Beijing 102205, PR China

[b]Beijing Institute of Pharmaceutical Chemistry, Beijing 102205, PR China

Contents

1. NMR and HR-MS spectra of RBNP and RBMP

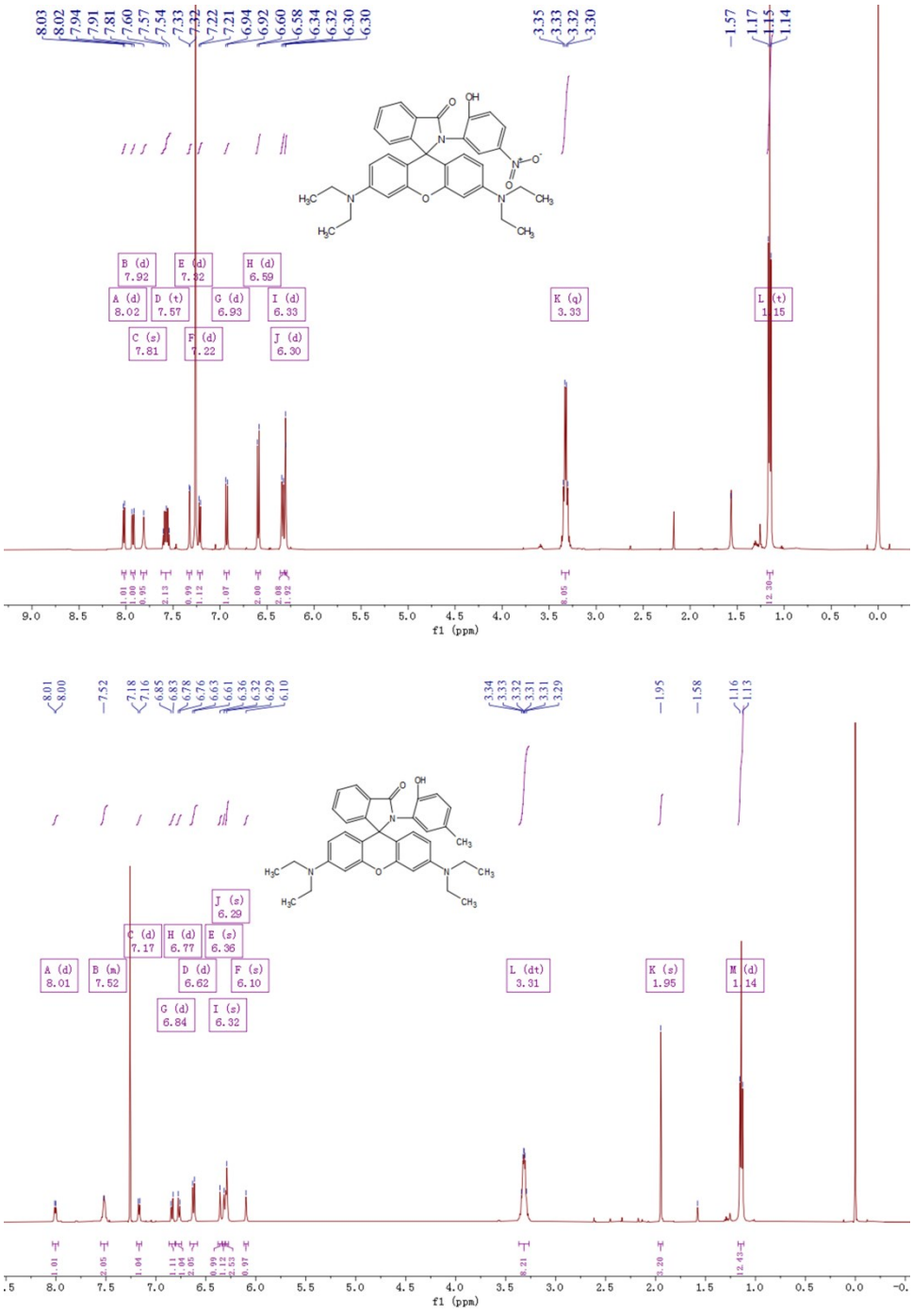

Fig. S1 ^{1}H NMR spectra of **RBNP** (up) and **RBMP** (down) in DMSO-d_6

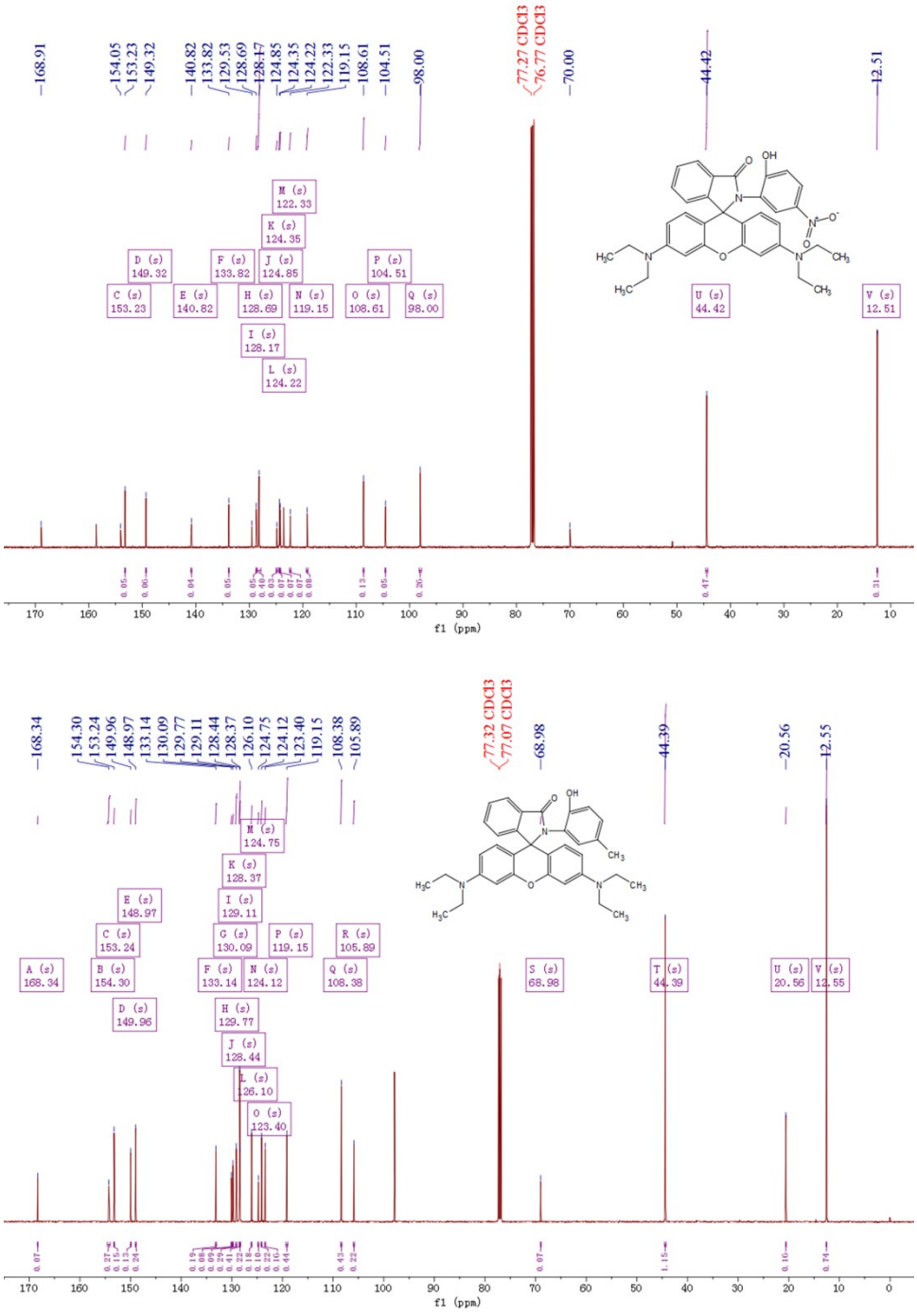

Fig. S2 ^{1}C NMR spectra of **RBNP** (up) and **RBMP** (down) in DMSO-d_6

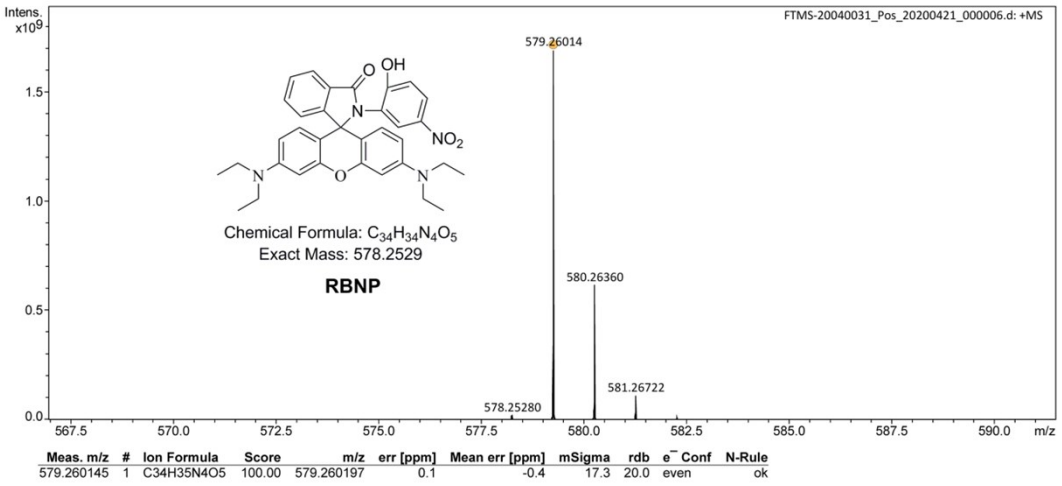

Meas. m/z	#	Ion Formula	Score	m/z	err [ppm]	Mean err [ppm]	mSigma	rdb	e⁻ Conf	N-Rule
579.260145	1	C34H35N4O5	100.00	579.260197	0.1	-0.4	17.3	20.0	even	ok

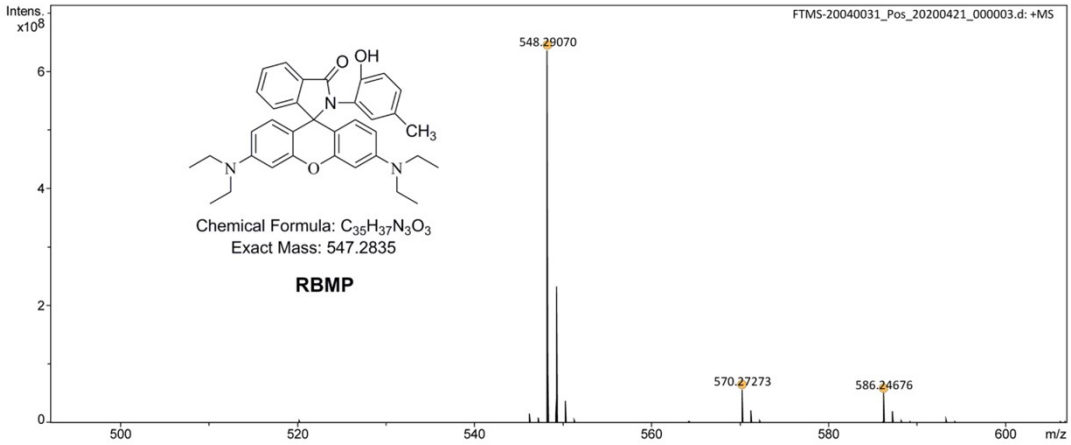

Meas. m/z	#	Ion Formula	Score	m/z	err [ppm]	Mean err [ppm]	mSigma	rdb	e⁻ Conf	N-Rule
548.290701	1	C35H38N3O3	100.00	548.290769	0.1	-0.2	21.3	19.0	even	ok
570.272734	1	C35H37N3NaO3	100.00	570.272713	-0.0	-0.3	14.8	19.0	even	ok
586.246763	1	C35H37KN3O3	100.00	586.246650	-0.2	-0.2	8.1	19.0	even	ok

Fig. S3 HR-MS spectra of **RBNP** (up) and **RBMP** (down)

2. Spectra for RBMP with DCP

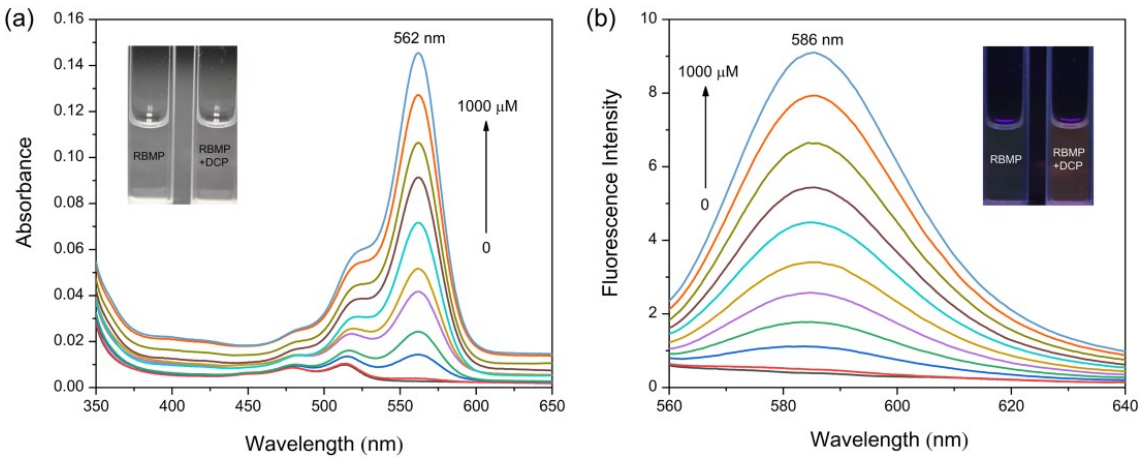

Fig. S4 (a) UV-Vis spectra of **RBMP** (100 μM) in DMF upon additions of DCP (1000 μM). Inset: The color change without and with the addition of DCP. (b) Fluorescence spectra of **RBMP** (50 μM) in DMF upon additions of DCP (1000 μM). Inset: The fluorescence change without and with the addition of DCP.

3. Limit of detection (LOD) for RBNP and RBMP with DCP

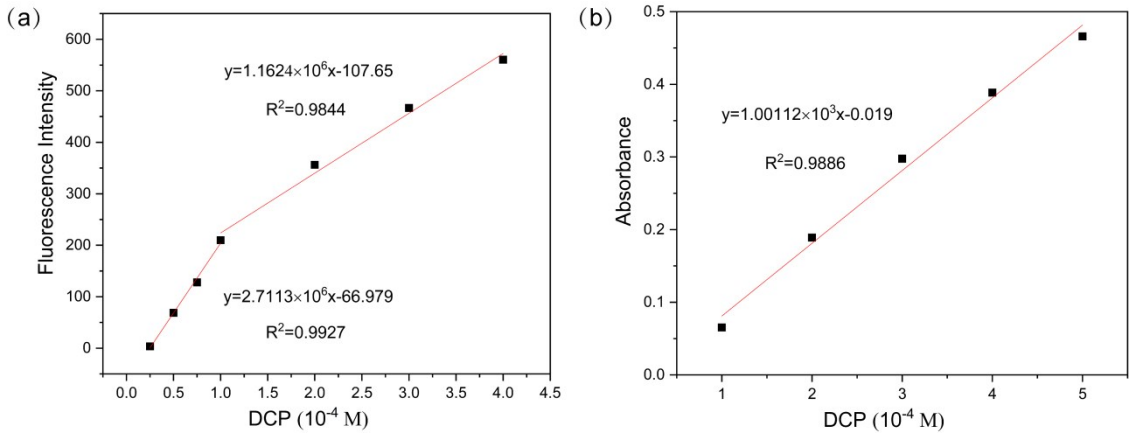

Fig. S5 (a) The plot of fluorescent intensity at 588 nm of **RBNP** with the concentration of DCP in DMF. (b) The plot of absorbance at 563 nm of **RBNP** with the concentration of DCP in DMF.

From **Fig. S5a**, the slope of the fitting curve k1 and k2 is respectively 2.7113×10^{6} and 1.1624×10^{6} in the DCP concentration of 0-1.0×10^{-4} M and 0-4.0×10^{-4} M. Then, according to the standard deviation of blank sample $\delta = 0.0013$ and the formula ($LOD = 3\delta/k$), the limit of detection (LOD) was calculated as 1.4×10^{-9} M (1.4 nM) and 3.3×10^{-9} M (3.3 nM) in the DCP concentration range of 0-1.0×10^{-4} M and 0-4.0×10^{-4} M.

From **Fig. S5b**, the slope of the fitting curve k is 1.001×10^{2} in the DCP concentration from 0 to 5.0×10^{-4} M. Then, according to the standard deviation of blank sample $\delta = 1.0\times10^{-4}$ and the formula ($LOD = 3\delta/k$), the limit of detection (LOD) was calculated as 3.1×10^{-7} M (0.31 μM) in the DCP concentration range of 0-5.0×10^{-4} M.

For the probe RBNP, the LOD of FL method was much lower than that of UV-Vis method in the DCP concentration range of 0-4.0×10^{-4} M.

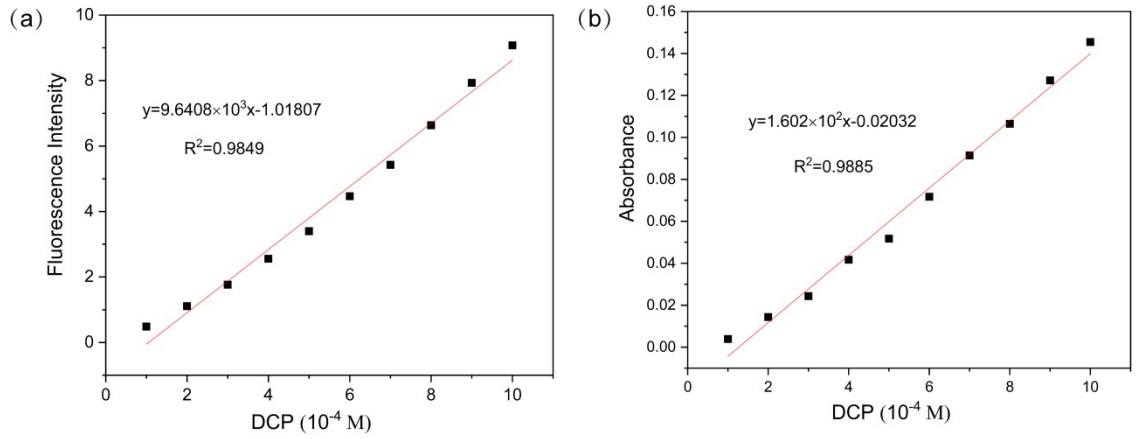

Fig. S6 (a) The plot of fluorescent intensity at 586 nm of **RBMP** with the concentration of DCP in DMF. (b) The plot of absorbance at 562 nm of **RBMP** with the concentration of DCP in DMF.

From **Fig. S6a**, the slope of the fitting curve k is 9.6408×10^3 in the DCP concentration from 0 to 10.0×10^{-4} M. Then, according to the standard deviation of blank sample δ = 0.0016 and the formula (LOD = 3δ/k), the limit of detection (LOD) was calculated as 5.0×10^{-7} M (0.5 μM) in the DCP concentration range of 0-1.0×10^{-4} M.

From **Fig. S6b**, the slope of the fitting curve k is 1.602×10^2 in the DCP concentration from 0 to 10.0×10^{-4} M. Then, according to the standard deviation of blank sample δ = 1.3×10^{-4} and the formula (LOD = 3δ/k), the limit of detection (LOD) was calculated as 2.4×10^{-6} M (2.4 μM) in the DCP concentration range of 0-1.0×10^{-4} M.

For the probe RBMP, the LOD of FL method was lower than that of UV-Vis method in the DCP concentration range of 0-1.0×10^{-4} M.

4. Kinetics Study

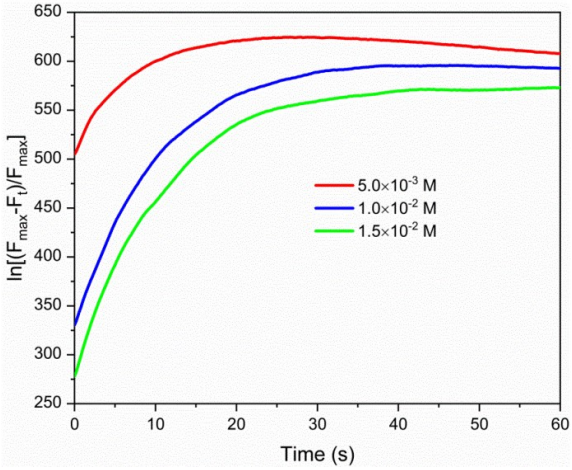

Fig. S7 Time-dependent fluorescence intensity of **RBNP** (50 μM) at 588 nm with the addition of DCP (5 mM, 10mM, 15mM).

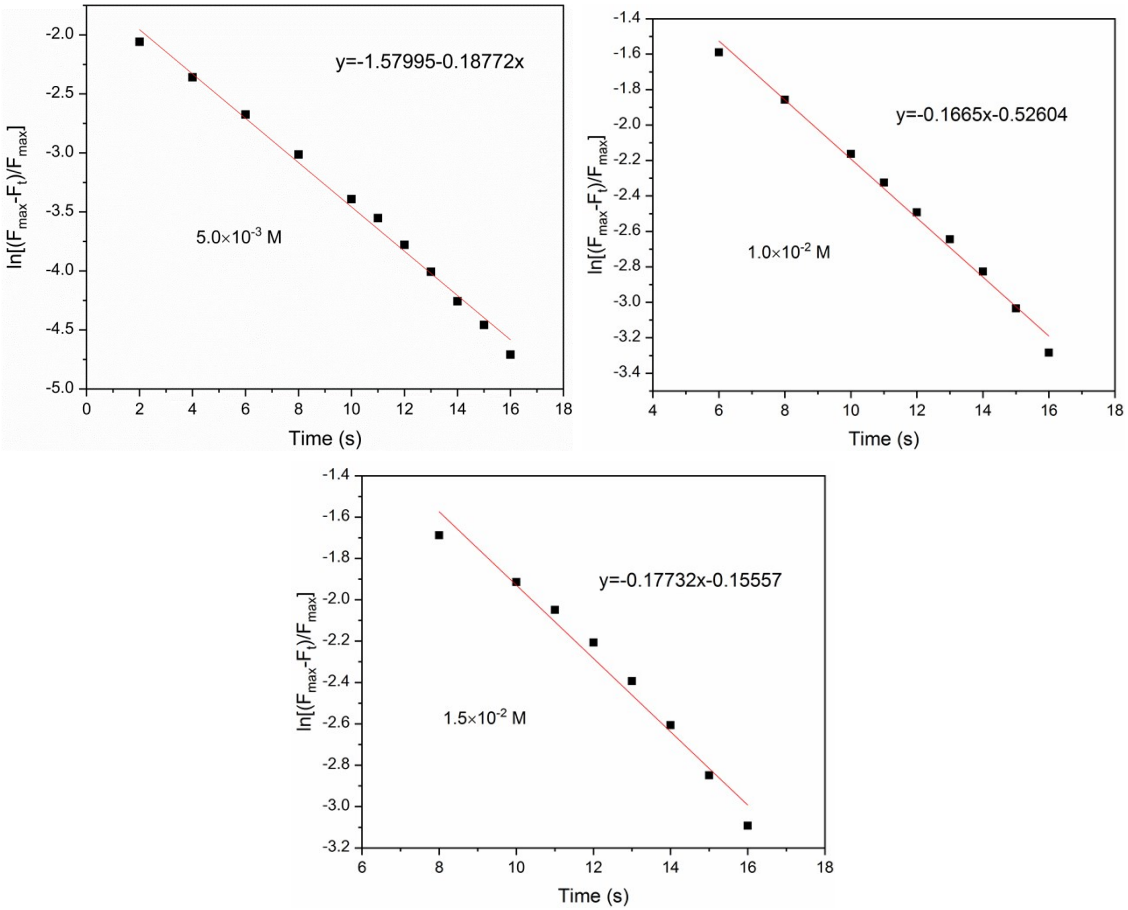

Fig. S8 Pseudo-first-order kinetic plots of reaction between **RBNP** (50 μM) and different concentrations of DCP (5 mM, 10mM, 15mM) in DMF.

5. Interference experiment

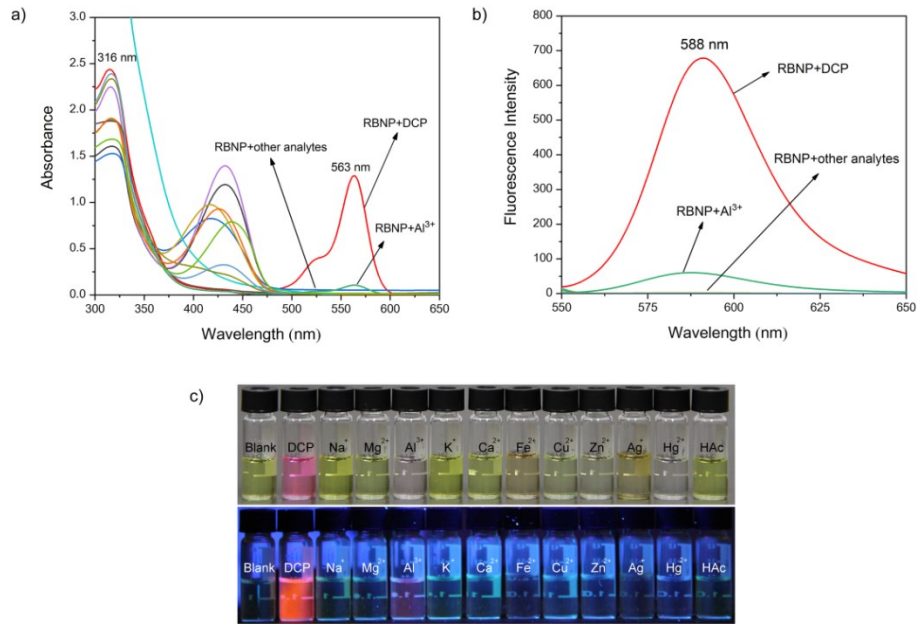

Fig. S9 UV-Vis absorption (a), fluorescent intensity (b) of **RBNP** with DCP, metal ion and HAc (10 equiv.). (c) The color changes of **RBNP** with DCP metal ion and HAc (10 equiv.) under sunlight (up) and 365nm UV light (down).

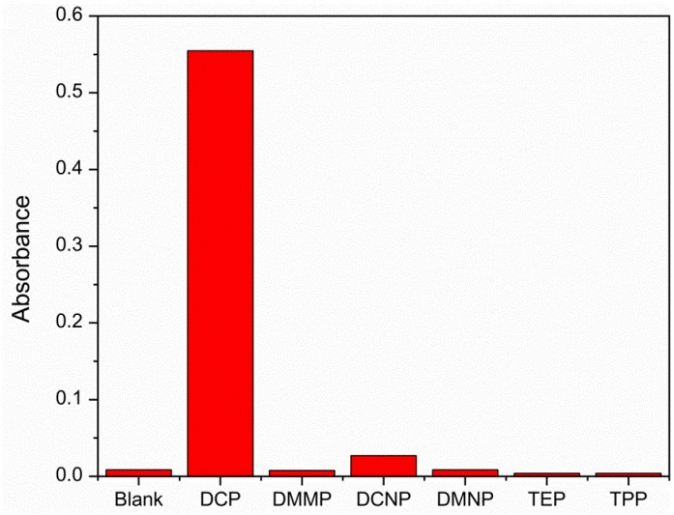

Fig. S10 UV-Vis absorption of **RBNP** (100 μM) to DCP (1000 μM) and other interferents (1000 μM).

6. Sensing mechnism

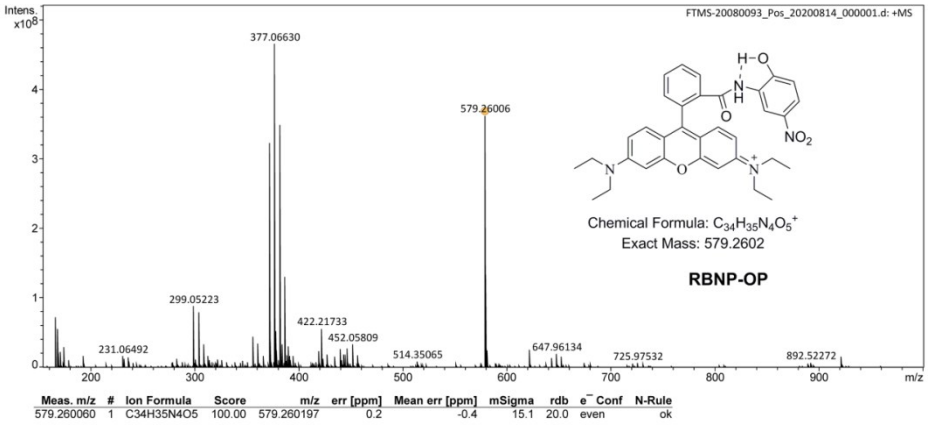

Fig. S11 HR-MS of **RBNP-OP**

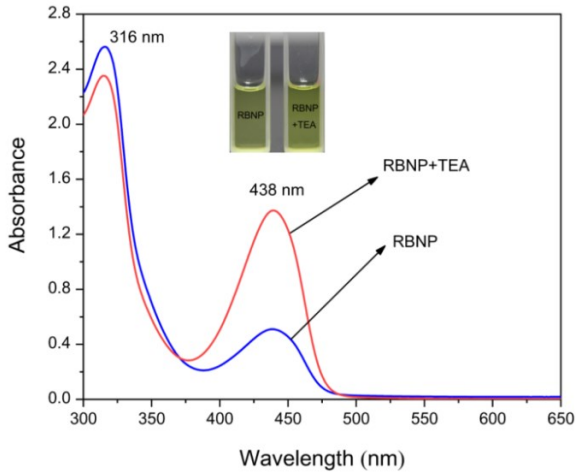

Fig. S12 UV-Vis spectra of **RBNP** (50 μM) in DMF without and with TEA (1000 μM). Inset: The color change without and with the addition of TEA.

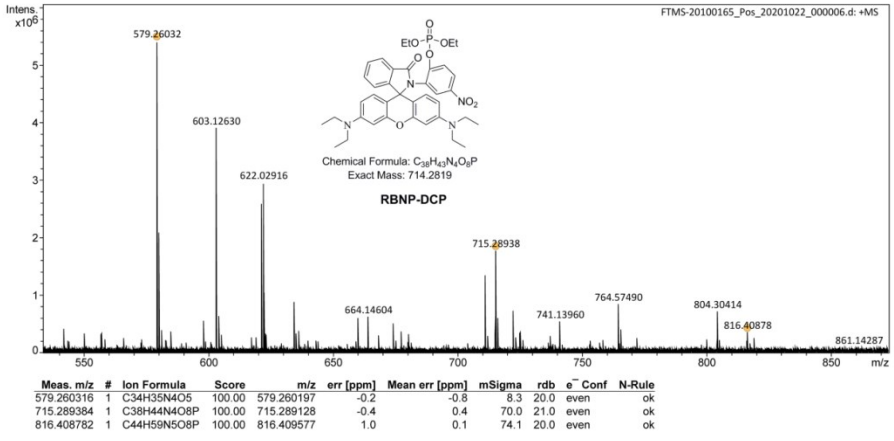

Fig. S13 HR-MS of **RBNP-DCP**

7. Theoretical Study

Table S1: Selected electronic transition energies (eV), oscillator strengths (f) and main orbital configurations of **RBNP** and **RBNP-OP**. [a] Only selected transition states were considered. The numbers in parentheses are the transition energy in wavelength. [b] Oscillator strength. [c] H stands for HOMO and L stands for LUMO.

Molecules	Electronic transition	Transition Energy[a]	f[b]	Composition[c]	(Composition) %
RBNP	$S_0 \rightarrow S_7$	3.8656eV 320.74nm	0.0191	H→L+2	97.2
	$S_0 \rightarrow S_8$	3.9619eV 312.94nm	0.1400	H-3→L, H-4→L	62.9, 23.6
RBNP-OP	$S_0 \rightarrow S_1$	2.5559eV 485.09nm	0.9583	H→L	98.4
	$S_1 \rightarrow S_0$	2.2906eV 541.27nm	1.1174	H→L	99.6

Table S2: Energies of the highest occupied molecular orbital (HOMO) and lowest unoccupied molecular orbital (LUMO) of **RBNP** and **RBNP-OP.**

Species	E_{HOMO}(a.u)	E_{LUMO}(a.u)	ΔE(a.u)	ΔE(eV)	ΔE(kJ/mol)
RBNP	-0.193131	-0.090331	0.102800	2.797327	269.901049
RBNP-OP	-0.210793	-0.108325	0.102468	2.788288	269.029001

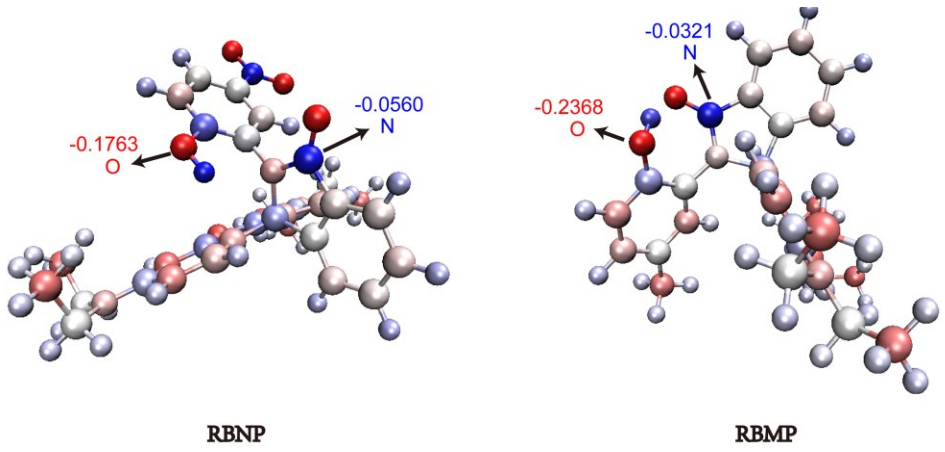

Fig. S14 Partial atomic charges of **RBNP** and **RBMP**

8. Comparision of this work and some reported DCP probes in the past five years.

Chemical structure	LOD for solution	Vapor detection		Visual detection for naked eye	Reference
		Concentration	Response time		
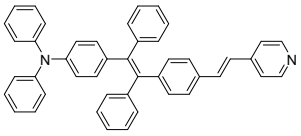	-	0.377 ppm	30 s	-	J. Mater. Chem. C 4 (2016) 10105-10110
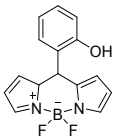	0.71 μg/L	132 ppm	3 s	-	Anal. Chem. 88 (2016) 9259-9263
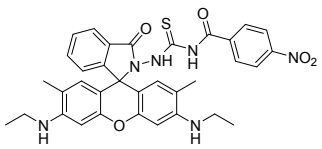	14.2 μM	-	-	colorless to pink	Sensors and Actuators B 235 (2016) 447-456
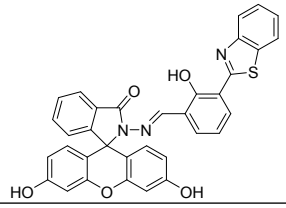	1.6 μM	-	-	Orange to cyan(UV-light)	New J. Chem. 41 (2017) 6661-6666
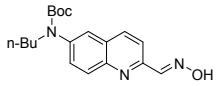	21 nM	130 ppm	5 min	white to yellow	J. Mater. Chem. C 5 (2017) 7337-7343
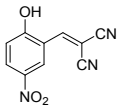	0.1 μM	50 ppm	1 min	colorless to light yellow	Analyst 143 (2018) 4171-4179
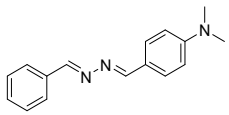	-	130 ppm	100 s	light yellow to yellow	ACS Sensors 3 (2018) 1445-1450
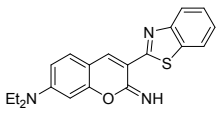	0.065 μM	-	-	green to light gold	Journal of Hazardous Materials 342 (2018) 10-19
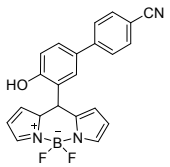	1.87 ppb	50 μM	3 s	-	Sensors and Actuators B 255 (2018) 176-182
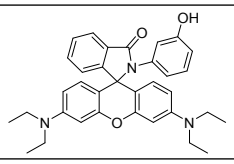	5.6 nM	-	30 s	colorless to deep pink	Scientific Reports 8 (2018) 3402

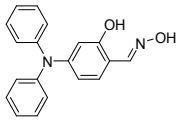	0.14 μM	10 μM	30 s	colorless to yellow	Dyes and Pigments 170 (2019) 107585
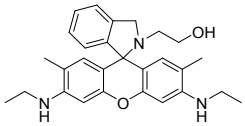	9.66 nM	-	-	colorless to pink	Dyes and Pigments 171 (2019) 107712
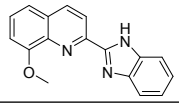	93.8 nM	6 ppm	60 s	colorless to light brown	New J. Chem. 43 (2019) 8627-8633
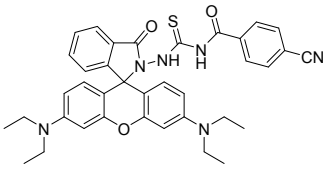	2 μM	DCP 20ppm GD 40 ppm	10min	colorless to pink	Molecules 24 (2019) 827
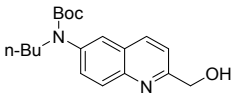	0.16 μM	130 ppm	20 s (fiber)	-	Sensors & Actuators B 318 (2020) 127937
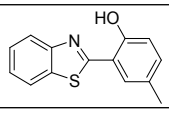	0.186 μM	100 ppm	2 min	-	Sensors & Actuators B 319 (2020) 128282
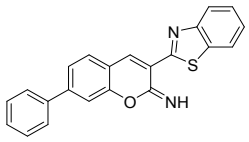	15.8 nM	100 ppm	60 s	-	Journal of Photochemistry & Photobiology A: Chemistry 388 (2020) 112188
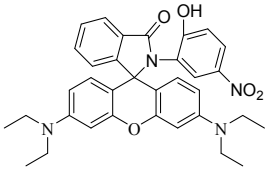	**1.4 nM**	**DCP 130 ppm GB 100 ppm**	**30 s**	**light yellow to pink**	**This work**